Ultrafast mantle impregnation by carbonatite melts

Tahar Hammouda*
Didier Laporte
Laboratoire Magmas et Volcans, Université Blaise Pascal and Centre National de la Recherche Scientifique, 5 rue Kessler, 63038 Clermont-Ferrand Cedex, France

ABSTRACT

Carbonatitic melts are often invoked as responsible for metasomatism in the mantle because of their unique chemical and physical properties. Here we report on infiltration experiments demonstrating that such melts can percolate very quickly in polycrystalline olivine. Carbonatites can travel over several millimeters in one hour and the infiltration rate is kinetically controlled by cation diffusion in the melt. The observed rates are several orders of magnitude higher than those previously found for basalt infiltration in mantle lithologies. Infiltration proceeds by a dissolution-precipitation mechanism wherein porosity is created in the dunite by dissolution of olivine at grain edges. This reaction is accompanied by forsterite reprecipitation in the carbonatite reservoir. Such a mechanism would likely favor chemical exchange between melt and matrix during percolation. We propose a migration model combining infiltration and compaction by which carbonatite melts can travel upward in the mantle over hundreds to thousands of meters on time scales of 0.1–1 m.y.

Keywords: mantle, metasomatism, carbonatite, infiltration, experimental, kinetics.

INTRODUCTION

There is much direct and indirect evidence that carbonatitic melts exist in the mantle (Green and Wallace, 1988; Yaxley et al., 1991; Hauri et al., 1993; Rudnick et al., 1993; Harmer and Gittings, 1998). Because they are not silicate they differ from the majority of natural melts formed in the Earth interior in terms of their physical (e.g., density, Genge et al., 1995; viscosity, Treiman, 1989) and chemical (e.g., major and trace element concentrations, Woolley and Kempe, 1989) properties. The origin of those melts and how they reach the Earth's surface is still being debated (Barker, 1989; Kjasgaard and Hamilton, 1989; Wyllie, 1989; Woolley et al., 1991; Green et al., 1993; Dalton and Wood, 1995; Wyllie and Lee, 1998). For petrologists and geochemists, carbonatite melts are of special interest because they combine good wetting properties (Hunter and McKenzie, 1989; Watson et al., 1990) and specific chemical signatures. This combination makes them a potentially powerful metasomatic agent because they are able to disseminate those elements they contain (i.e., rare earth elements, Rb, K, Na, Ba, Sr, Nb, Ta, Zr, U, Th, P) while passing through mantle lithologies (e.g., McKenzie, 1985).

Because the dihedral angles measured at the contact of carbonate melts and silicate minerals are much lower than 60° (Hunter and McKenzie, 1989; Watson et al., 1990), interfacial energy-driven infiltration (Watson, 1982; Stevenson, 1986) is one mechanism by which mantle rocks could be impregnated by carbonatites on a large scale. Whereas much attention has been paid in the past to the infiltration of basaltic melts in peridotites (Watson, 1982; Riley and Kohlstedt, 1990; Daines and Kohlstedt, 1994), the infiltration behavior of carbonatite melts has never been investigated despite their unique chemical properties. Here we report on high-pressure experiments designed to determine the infiltration rate of carbonatites in mantle lithologies, and to characterize the mechanisms involved in this process.

EXPERIMENTS

Infiltration experiments were performed at 10 kbar and 1300 °C on couples consisting of a synthetic dunite placed against a carbonatite reservoir made of sodium carbonate saturated with forsterite at experimental conditions. The dunite was prepared separately, by sintering synthetic forsterite crystals sieved to 20 µm in a piston cylinder apparatus at 10 kbar and 1100 °C for 5 days. Initial porosity in the synthetic dunite was restricted to rare isolated voids at grain edges. We chose sodium carbonate for the carbonatite because it is a good analogue for natural carbonatite compositions when considering physical properties such as viscosity or wetting behavior (Treiman, 1989; Watson et al., 1990). The carbonate melt was saturated in forsterite by adding MgO and SiO_2 to the carbonate in quantities determined by earlier saturation experiments. We found that 16 wt% of forsterite could be dissolved in the sodium carbonate at 10 kbar and 1300 °C. Using such a melt composition ensured that infiltration was the response to the sole minimization

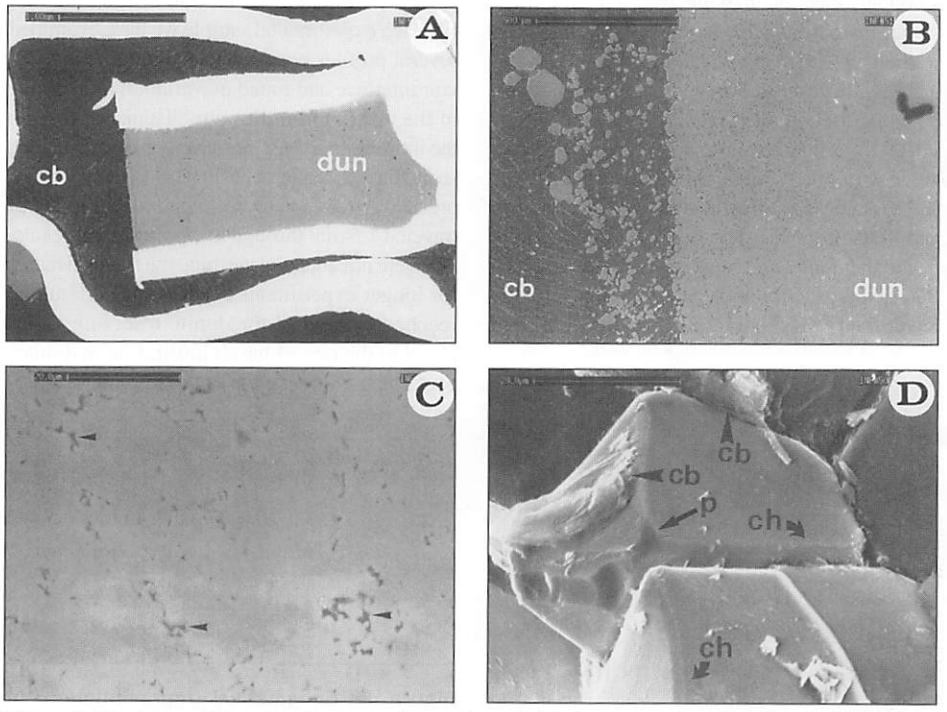

Figure 1. Electron microscope images of experimental textures produced during infiltration of dunite by carbonate melt at 1300 °C and 10 kbar. A: General view of infiltration couple (sample INF57); carbonatite reservoir (cb) was positioned on top and dunite (dun) was at bottom. Bright material is platinum used to contain samples. Scale bar is 1 mm. B: Closer view of infiltrated dunite (sample INF51); quenched carbonate melt pockets are present between grains of dunite and euhedral forsterite crystals have grown in carbonatite reservoir next to dunite contact. Scale bar is 500 µm. C: Smaller quenched carbonate melt pockets (arrows) can be found farther inside percolated dunite (sample INF58, 200 µm from carbonatite reservoir). Scale bar is 20 µm. D: Detail of carbonatite-forsterite wetting textures (sample INF50) showing melt channels (ch) along grain edges, melt pockets (p) at grain corners, and quenched carbonate melt. Scale bar is 20 µm.

*Present address: Geochemisches Institut, Universität Göttingen, Goldschmidtstrasse 1, 37077 Göttingen, Germany. E-mail: taharh@ugcvax.dnet.gwdg.de.

TABLE 1. MELT INFILTRATION DISTANCES OF CARBONATITE AND BASALT MEASURED IN THE EXPERIMENTAL SAMPLES

Run#	Melt	Pressure (kbar)	Temperature (°C)	Time (min)	Infiltration distance (mm)
INF57	Carbonatite	10	1300	10	0.8
INF58	Carbonatite	10	1300	30	1.8
INF56	Carbonatite	10	1300	60	2.5
INF51	Carbonatite	10	1300	150	Complete impregnation
INF50	Carbonatite	10	1300	5700	Complete impregnation
INF30	Basalt	10	1290	7290	0.1
INF34	Basalt	10	1290	8340	0.2

of interfacial energies of the system (Watson, 1982). The carbonate was placed on top of the dunite in a platinum capsule, and the couples were run vertically in a piston-cylinder apparatus.

CARBONATITE INFILTRATION RATES

In Figure 1 we show the experimental setup and the resulting infiltration textures. Although less dense and positioned at the top of the couple, the carbonatite melt penetrated the dunite. During the experiments the boundary between the two media remained stationary. Polished sections of the dunite reveal distinct melt pockets at olivine trijunctions corresponding to the intersection of melt channels along olivine grain edges. The pockets are larger and more numerous near the interface, but they can also be seen farther inside the dunite. A higher magnification view using secondary electron imaging gives a three-dimensional insight into the geometry of carbonatite wetting, with melt tubules along grain edges joining at grain corners. The volume fraction of carbonatitic melt in the dunite near the interface is ≈0.18, in fair agreement with the equilibrium value computed for a dihedral angle of 30° (0.18–0.25 depending on grain shape; Laporte and Watson, 1995). The porosity drops rapidly inside the dunite and most of the infiltrated portion displays carbonatite melt volume fraction lower than 0.01. No significant forsterite grain coarsening was associated with infiltration despite the much higher temperature compared to dunite synthesis conditions.

An important feature of Figure 1 is that a layer of newly formed euhedral forsterite crystals is present in the carbonatite reservoir next to the dunite-carbonatite boundary. Those crystals have precipitated in the melt, in response to the dissolution of forsterite along grain edges in the dunite. Because the melt is initially saturated in forsterite the material dissolved in the aggregate cannot stay in the melt and mass balance requires that it is released somewhere in the system.

We have performed several infiltration experiments at the same run conditions with different durations (Table 1). In Figure 2 we plot the maximum carbonatite infiltration distance measured on electron microscope photomicrographs for each experiment as a function of run duration. For each experimental sample we have examined several profiles normal to the dunite-melt reservoir interface and found no variation in the value of the maximum infiltration distance, although the infiltration front is not strictly planar. It can be seen that carbonatite infiltration is a very fast process. After 1 hr at run conditions, the melt has traveled 2.5 mm through the forsterite aggregate. We were not able to determine the travel distance for longer experiments because the carbonatite reached the end of the dunite reservoir. Compared to the rate of basalt infiltration in dunites performed following the same experimental procedure (1 mm or less per day, Watson, 1982; Daines and Kohlstedt, 1994; and our data in Table 1), the infiltration rates are orders of magnitude higher for carbonatites. When plotted against the square root of time, the penetration distance of the carbonatite melt displays a linear relationship. This suggests that the melt infiltration is governed by a diffusion-type rate law $x = \sqrt{Dt}$, where x is the infiltration distance, t is time, and D is a diffusion coefficient relevant to the infiltration process. Regression of the data yields $D \approx 1.8 \cdot 10^{-9} m^2 s^{-1}$. This value is of the order of what we can anticipate for cation diffusivities in carbonatitic liquids (Spedding and Mills, 1985; Treiman, 1989).

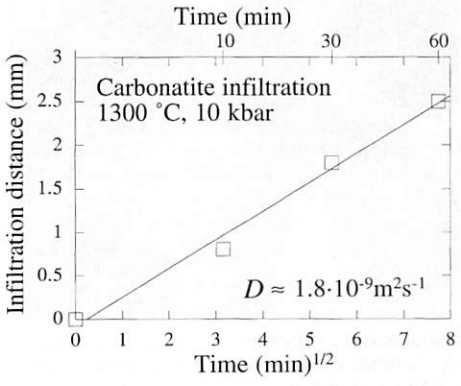

Figure 2. Infiltration distance of carbonate melt in synthetic dunite at 1300 °C and 10 kbar as function of time (upper scale) and square root of time (lower scale). Linear relationship of distance when expressed as function of square root of time indicates diffusion type kinetic law with $D = 1.8 \cdot 10^{-9} m^2 s^{-1}$.

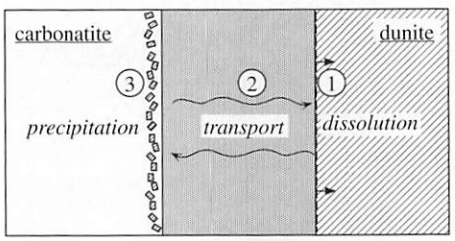

Figure 3. Schematical representation of processes involved during carbonatite infiltration in synthetic dunite: (1) dissolution occurs ahead of infiltration front in order to create porosity and allow melt advance; (2) dissolved material is transported by diffusion in part of dunite already impregnated toward carbonatite reservoir; (3) when reaching carbonatite reservoir material is precipitated, causing forsterite growth in region next to boundary between dunite and carbonatite.

CARBONATITE INFILTRATION MECHANISM

By combining the different observations we are able to deduce that carbonatite infiltration proceeds by a dissolution-precipitation mechanism. The best argument is the precipitation of forsterite in the carbonatite reservoir next to the infiltrated dunite. Such a mechanism was suggested by Watson (1982) for basalt infiltration in dunites but experimental evidence was lacking. The interpretation of the current infiltration experiments is sketched in Figure 3. Carbonatite infiltration in the silicate matrix involves three major steps: (1) forsterite dissolution proceeds ahead of an infiltration front and results in the formation of an interconnected network of carbonate melt channels along grain edges; (2) the dissolved material is then transported by diffusion in the melt toward the carbonatite reservoir, through the portion of the couple that has already been infiltrated by the carbonatite; and (3) forsterite precipitation (in an amount equal to the amount dissolved at the infiltration front) occurs back in the reservoir. The linear relationship between the infiltration distance and the square root of time indicates that atomic diffusion in the carbonatite melt is the rate-limiting process. Therefore, grain size is expected to be unimportant for controlling infiltration rate because the effective diffusion coefficient in partially molten systems depends on melt geometry (through a tortuosity factor) and melt fraction, but not on grain size.

IMPLICATIONS FOR CARBONATITE METASOMATISM AND MAGMATISM

A consequence of the penetrative infiltration mechanism observed in the experiments is that chemical exchange between melt and matrix is favored. Here, we chose a protocol such that there was always chemical equilibrium between melt and matrix in order to simplify the texture interpretations. If the carbonatite and the silicate matrix were not at chemical equilibrium, as would be the case in the mantle, dissolution and precipitation reactions would result in a very efficient exchange of components (including trace elements and isotopes) between the melt and the

matrix in addition to carbonate and apatite precipitation or mineral replacement, such as that of orthopyroxene by clinopyroxene. Studies of mantle xenoliths from continental as well as oceanic environments document reactions of this type (Green and Wallace, 1988; Yaxley et al., 1991; Hauri et al., 1993; Rudnick et al., 1993; Coltorti et al., 1999). Such interaction could result from the migration of carbonatite melts either directly from their production regions, or from dikelets that could have traveled short distances. From our experiments, we can calculate that on the time scale of 10 k.y. to 1 m.y. carbonatitic melts can metasomatize regions extending tens to hundreds of meters from their source simply by interfacial energy-driven infiltration. However, this process requires the affected mantle to be above the carbonated solidus, otherwise the melt would freeze.

If we now take into account the effect of gravity-driven compaction migration distances can be increased significantly. Once a region of the mantle has been impregnated by carbonate melt it can be subjected to compaction. Using equation 15 of Stevenson (1986), we find that compaction will proceed once the impregnated region has reached a vertical thickness of 1–10 m for porosity of 0.01–0.001, respectively. For smaller thicknesses interfacial energies are more important than gravity and may prevent compaction. We can therefore envision a carbonatite migration model in the mantle wherein infiltration operates ahead and rapidly leads to the establishment of an interconnected porosity over a short distance (to a few tens of meters), while compaction operates behind to concentrate the carbonatite melt below the infiltration front. The infiltration-compaction model results in migration rates faster than a simple diffusion-controlled infiltration mechanism. A simple calculation using McKenzie's (1985) equations for compaction and our experimental data for infiltration suggests that carbonatite melts could travel upward over hundreds to thousands of meters for time scales of 100 k.y. to 1 m.y. The same calculations for basalts show that diffusion-controlled infiltration, even when coupled with compaction, is ineffective because diffusion in basaltic melt is so small.

An important result gathered from our experiments is that carbonatite melts will naturally tend to disseminate in the surrounding mantle, which is the opposite of what is needed for magma segregation and pooling. Even if compaction occurs, the amounts of melts concerned will remain small because segregated melts will tend to disperse again. Therefore carbonate melts will tend to remain stored in the mantle, which, together with low carbon contents in the mantle, might explain their scarcity in nature (Woolley, 1989). Carbonatitic magmatism could arise from partial melting of regions of the mantle that have already been impregnated by repeated previous carbonatite fluxes. Low-degree melting of those affected zones would then produce sufficient amounts of carbonatite magma that can be segregated and reach shallow levels. A higher degree of melting of carbon-enriched mantle lithologies will produce alkalic lavas (Wallace and Green, 1988; Dalton and Presnall, 1998) that could bear a strong (enriched) geochemical signature inherited from earlier carbonatite circulation in their source region (Norry and Fitton, 1983).

ACKNOWLEDGMENTS

We thank Hiroko Nagahara for providing us with the synthetic forsterite crystals used in the experiments. Insightful comments by M. J. Walter and D. R. Lentz were very helpful. This work was financially supported by the Institut National des Sciences de l'Univers (Centre National de la Recherche Scientifique).

REFERENCES CITED

Barker, D. S., 1989, Field relations of carbonatites, *in* Bell, K., ed., Carbonatites: Genesis and evolution: London, Unwin Hyman, p. 38–69.

Coltorti, M., Bonadiman, C., Hinton, R. W., Siena, F., and Upton, B. G. J., 1999, Carbonatite metasomatism of the oceanic upper mantle: Evidence from clinopyroxenes and glasses in ultramafic xenoliths of Grande Comore, Indian Ocean: Journal of Petrology, v. 40, p. 133–165.

Daines, M. J., and Kohlstedt, D. L., 1994, The transition from porous to channelized flow due to melt/rock reaction during melt migration: Geophysical Research Letters, v. 21, p. 145–148.

Dalton, J. A., and Presnall, D. C., 1998, The continuum of primary carbonatitic-kimberlitic melt compositions in equilibrium with lherzolite: Data from the system CaO-MgO-Al_2O_3-SiO_2-CO_2 at 6 GPa: Journal of Petrology, v. 39, p. 1953–1964.

Dalton, J. A., and Wood, B. J., 1995, The stability of carbonate under upper-mantle conditions as a function of temperature and oxygen fugacity: European Journal of Mineralogy, v. 7, p. 883–891.

Genge, M. J., Price, G. D., and Jones, A. P., 1995, Molecular dynamics simulations of $CaCO_3$ melts to mantle pressures and temperatures: Implications for carbonatite magmas: Earth and Planetary Science Letters, v. 131, p. 225–238.

Green, D. H., and Wallace, M. E., 1988, Mantle metasomatism by ephemeral carbonatite melts: Nature, v. 336, p. 459–462.

Green, D. H., Eggins, S. M., and Yaxley, G., 1993, The other carbon cycle: Nature, v. 365, p. 210–211.

Harmer, R. E., and Gittins, J., 1998, The case for primary, mantle-derived carbonatite magma: Journal of Petrology, v. 39, p. 1895–1903.

Hauri, E. H., Shimizu, N., Dieu, J. J., and Hart, S. R., 1993, Evidence for hotspot-related carbonatite metasomatism in the oceanic upper mantle: Nature, v. 365, p. 221–227.

Hunter, R. S., and McKenzie, D., 1989, The equilibrium geometry of carbonate melts in rocks of mantle composition: Earth and Planetary Science Letters, v. 92, p. 347–356.

Kjarsgaard, B. A., and Hamilton, D. L., 1989, The genesis of carbonatites by immiscibility, *in* Bell, K., ed., Carbonatites: Genesis and evolution: London, Unwin Hyman, p. 388–404.

Laporte, D., and Watson, E. B., 1995, Experimental and theoretical constraints on melt distribution in crustal sources: The effects of crystalline anisotropy on melt interconnectivity: Chemical Geology, v. 124, p. 161–184.

McKenzie, D., 1985, The extraction of magma from the crust and mantle: Earth and Planetary Science Letters, v. 74, p. 81–91.

Norry, M. J., and Fitton, J. G., 1983, Compositional differences between oceanic and continental basic lavas and their significance, *in* Hawkesworth, C. J., and Norry, M. J., eds., Continental basalts and mantle xenoliths: Nantwich, Shiva Geology Series, p. 5–19.

Riley, G. N., and Kohlstedt, D. L., 1990, Melt migration in a silicate liquid-olivine system: An experimental test of compaction theory: Geophysical Research Letters, v. 17, p. 2101–2104.

Rudnick, R. L., McDonough, W. F., and Chappell, B. W., 1993, Carbonatite metasomatism in the northern Tanzanian mantle: Petrographic and geochemical characteristics: Earth and Planetary Science Letters, v. 114, p. 463–475.

Spedding, P. L., and Mills, R., 1985, Trace-ion diffusion in molten alkali carbonates: Journal of the Electrochemical Properties, v. 112, p. 594–599.

Stevenson, D. J., 1986, On the role of surface tension in the migration of melts and fluids: Geophysical Research Letters, v. 13, p. 1149–1152.

Treiman, A. H., 1989, Carbonatite magma: Properties and processes, *in* Bell, K., ed., Carbonatites: Genesis and evolution: London, Unwin Hyman, p. 89–104.

Wallace, M. E., and Green, D. H., 1988, An experimental determination of primary carbonatite magma composition: Nature, v. 335, p. 343–346.

Watson, E. B., 1982, Melt infiltration and magma evolution: Geology, v. 10, p. 236–240.

Watson, E. B., Brenan, J. M., and Baker, D. R., 1990, Distribution of fluids in the continental mantle, *in* Menzies, M. A., ed., Continental mantle: Oxford Monographs on Geology and Geophysics 16, p. 111–125.

Woolley, A. R., 1989, The spatial and temporal distribution of carbonatites, *in* Bell, K., ed., Carbonatites: Genesis and evolution: London, Unwin Hyman, p. 15–37.

Woolley, A. R., and Kempe, D. R. C., 1989, Carbonatites: Nomenclature, average chemical compositions, and element distribution, *in* Bell, K., ed., Carbonatites: Genesis and evolution: London, Unwin Hyman, p. 1–14.

Woolley, A. R., Barr, M. W. C., Din, V. K., Jones, G. C., Wall, F., and Williams, C. T., 1991, Extrusive carbonatites from the Uyaynah area, United Arab Emirates: Journal of Petrology, v. 32, p. 1143–1167.

Wyllie, P. J., 1989, Origin of carbonatites: Evidence from phase equilibrium studies, *in* Bell, K., ed., Carbonatites: Genesis and evolution: London, Unwin Hyman, p. 500–545.

Wyllie, P. J., and Lee, W.-J., 1998, Model system controls on conditions for formation of magnesiocarbonatite and calciocarbonatite magmas from the mantle: Journal of Petrology, v. 39, p. 1885–1893.

Yaxley, G. M., Crawford, A. J., and Green, D. H., 1991, Evidence for carbonatite metasomatism in spinel peridotite xenoliths from western Victoria, Australia: Earth and Planetary Science Letters, v. 107, p. 305–317.

Manuscript received August 2, 1999
Revised manuscript received November 24, 1999
Manuscript accepted December 7, 1999

Revised age of the Rockland tephra, northern California: Implications for climate and stratigraphic reconstructions in the western United States: Comment and Reply

COMMENT

A. M. Sarna-Wojcicki*
U.S. Geological Survey, MS 975, Menlo Park, California 94025, USA

Lanphere et al. (1999) presented new data for the age of the Rockland pumice tuff breccia of Wilson (1961) using the incremental-heating $^{40}Ar/^{39}Ar$ technique. Their age, ~610 ka, is ~200 ka older than zircon fission-track ages obtained on this tuff by Meyer et al. (1980; 1991). Application of new $^{40}Ar/^{39}Ar$ technologies to tephrochronometry is an important advance that allows more precise dating of widespread tephra layers. Although the new age may be correct, I urge caution in accepting it in place of grain-discrete fission-track dates and other data that suggest a younger age for this unit.

The Rockland tephra has proved difficult to date due to detrital and xenocrystic contamination. Meyer et al. (1980; 1991) chose a grain-discrete technique to circumvent this problem. Their study yielded combined zircon fission-track ages of 370 ± 50 ka and 400 ± 50 ka (~40 grains) on proximal sites, and 420 ± 80 ka and 460 ± 90 ka (~220 grains) on distal sites.

Meyer et al. (1980; 1991) identified zircon crystals that were rounded, had different color than the main zircon population, or lacked glass coats. Ages for these grains ranged from 0.39 Ma to 154 Ma. Meyer et al. (1980; 1991) also found physically distinct minor populations of zircon samples that yielded older ages: 570 ± 80 ka; 660 ± 110 ka; and single grains with anomalously high U contents yielding ages of 580 ka and 1.15 Ma. These grains were considered detrital or xenocrystic, and were not included in the age calculation.

Lanphere et al. (1999) faulted Meyer et al. (1991) for being too partial to the younger dates in citing the literature, and point to a 0.56 Ma age on volcanic glass shards cited in Izett (1981). This age was not cited by Meyer et al. (1991) because uncorrected fission-track ages on volcanic glass tend to be unreliable (Naeser et al., 1980). Meyer et al. (1980; 1991) presented results of 15 combined zircon fission-track ages, as well as older average fission-track ages of anomalous populations of zircon grains as discussed above. The latter ages are as old or older than the single 0.56 Ma age on glass cited in Izett (1981). Because all the latter determinations were on zircon grains, they were not subject to track fading, as would be expected in glass. In this regard, also note that Alloway et al. (1992) obtained an average age of 470 ± 40 ka on the Rockland pumice tuff breccia using the isothermal plateau fission-track (ITPFT) method on glass, a technique that compensates for track fading or annealing.

Lanphere et al. (1999) alleged that the fission-track counting technique used by Meyer et al. (1980; 1991) resulted in inaccurate, young fission-track ages, because it included induced-track counts from grains without fossil tracks in the age calculations. Some workers consider such grains to result from underetching. Three lines of evidence indicate that the counting method was appropriate. First, the number of grains containing no tracks was about the same as those containing one track or those that contained two tracks. This suggested that the unit was so young, and the uranium content so low, that some grains did not show fossil tracks because none had formed. Second, standards of known age that were run at the same time as the Rockland tephra utilizing identical etching and counting techniques were within analytical errors of ages obtained by other workers and by other techniques. Third, zircon grains from proximal sites were generally larger and had a larger number of fossil tracks than zircon grains from distal sites, indicating that frequency of fossil tracks was related to surface area and to the probability of acquiring fossil tracks as a function of grain size and time, not to efficiency of etching.

Data obtained from the Owens Lake core (Smith and Bischoff, 1997), provide an interpolated age of 510 ka for the Dibekulewe ash bed, an ash that stratigraphically underlies the Rockland ash bed, providing a maximum age estimate for the Rockland. In addition, multiple, mature soil profiles are present between the Lava Creek B and the Rockland ash beds at several sites, suggesting that a long period of time, ~100 ka, had elapsed between the deposition of these two units.

Lanphere et al. (1999) employed the incremental-heating $^{40}Ar/^{39}Ar$ technique that requires fusing a sample of several hundred grains or more, not a grain-discrete technique. The possibility that xenocrysts or "protocrysts" were included in the separate cannot be ruled out. For example, plagioclase, sanidine, and quartz grains with glass inclusions are present in the Bishop Tuff and ash. Although the sanidine grains generally yield coherent ages (~760 ka by laser-fusion $^{40}Ar/^{39}Ar$ analysis of single grains), individual plagioclase grains yield some older ages (for example 1.01 ± 0.01 Ma). Bogaard and Schirnick (1994) showed that comagmatic quartz crystals with K-rich glass inclusions in the Bishop Tuff were protocrysts, yielding an older age of 1.89 ± 0.03 Ma. .

Lastly, we find the supporting evidence for an older age of the Rockland pumice tuff breccia presented in Lanphere et al. (1999), based on the paleomagnetic direction of the andesitic basalt of Hootman Ranch and its correlation to the Big Lost Reversal Polarity Subchron, to be weak. The basalt's transitional paleomagnetic direction does not meet the definition of a reversed polarity, and could just as easily be correlated to any one of a number of younger magnetic excursions of Brunhes age. In conclusion, additional work needs to be done to provide a more secure age for the Rockland tephra.

REFERENCES CITED

Alloway, B. V., Westgate, J. A., Sandhu, A. S., and Bright, R. C., 1992, Isothermal plateau fission-track age and revised distribution of the widespread mid-Pleistocene Rockland tephra in west-central United States: Geophysical Research Letters, v. 19, p. 569–572.

Bogaard, P. V. D., and Schirnick, C., 1994, Single crystal $^{40}Ar/^{39}Ar$ ages of quartz protocrysts in the 0.761 Ma Bishop Tuff rhyolite (Long Valley, United States): ICOG-8, U.S. Geological Survey Circular 1107, 32 p.

Izett, G. A., 1981, Volcanic ash beds: Recorders of upper Cenozoic silicic pyroclastic volcanism in the western United States: Journal of Geophysical Research, v. 86, p. 10,200–10,222.

Lanphere, M. A., Champion, D. E., Clynne, M. A., and Muffler, L. J. P., 1999, Revised age of the Rockland tephra, northern California: Implications for climate and stratigraphic reconstructions in the western United States: Geology, v. 27, p. 135–138.

Meyer, C. E., Woodward, M. J., Sarna-Wojcicki, A. M., and Naeser, C. W., 1980, Zircon fission-track age of 0.45 million years on ash in the type section of the Merced Formation, west-central California: U.S. Geological Survey Open-File Report 80-1071, 9 p.

Meyer, C. E., Sarna-Wojcicki, A. M., Hillhouse, J. W., Woodward, M. J., Slate, J. L., and Sorg, D. H., 1991, Fission-track age (400,000 yr) of the Rockland tephra, based on inclusion of zircon grains lacking fossil fission tracks: Quaternary Research, v. 35, p. 367–382.

Naeser, C. W., Izett, G. A., and Obradovich, J. D., 1980, Fission-track and K-Ar ages of natural glasses: U.S. Geological Survey Bulletin 1489, 31 p.

Smith, G. I., and Bischoff, J. L., editors, 1997, An 800,000-year paleoclimatic record from core OL-92, Owens Lake, southeast California: Geological Society of America Special Paper 317, 165 p.

Wilson, T. A., 1961, The geology near Mineral, California [Master's thesis]: Berkeley, University of California, 75 p.

*Email: asarna@isdmnl.wr.usgs.gov.